Coal features and depositional environment of the Northern Karapınar–Ayrancı coal deposit (Konya, Central Turkey)

Rıza Görkem OSKAY[1] , Kimon CHRISTANIS[1,]* , Mert SALMAN[2]
[1]Department of Geology, University of Patras, Rio-Patras, Greece
[2]General Directorate of Mineral Research and Exploration (MTA), Ankara, Turkey

Abstract: The Karapınar–Ayrancı deposit is the most significant one among the recently explored coal deposits in Turkey. The aim of the present study was to determine maceral, mineralogical, and elemental compositions of coal samples picked up from one borehole (DK-7) drilled at the northern part of the deposit. The coal samples display moderate to high ash yield (average 38.7%, on dry basis), high volatile matter yield (average 33.9%, on dry basis), high total sulfur (average 6.7%, on dry basis) and low hydrogen contents (average 4.8%, dry basis). Huminite is dominant, and liptinite and inertinite appear at low concentrations. The bulk coal samples contain mainly quartz, clay minerals (mainly illite and chlorite), muscovite, feldspars, carbonates (calcite and aragonite), and rarely pyrite and gypsum/bassanite. The maceral and mineralogical compositions point to mesotrophic and rheotrophic conditions during peat accumulation; nevertheless, the inorganic intercalations show that peat formation was ceased several times. The petrographical and mineralogical compositions of coal seams in northern and eastern parts of the deposit could imply vegetation and water chemistry differences. The abundance of fossil shell-bearing layers in the studied samples could imply a slightly higher water table than this in the eastern part. In addition, higher telohuminite content might be related to a higher contribution of tree/bush peat-forming vegetation in the northern part; however, the lack of xylite-rich lithotype and the abundance of fluorinite-type resinite imply the predominance of shrubs on the palaeomire's surface. Overall, the precursor peat in the northern part of the deposit was accumulated under pure telmatic to limnotelmatic conditions, vegetation heterogeneity and ditches transporting inorganic material from the margins were developed on the surface of the Karapınar–Ayrancı paleomire.

Key words: Karapınar–Ayrancı, maceral composition, coal, peat-forming environment, coal facies, Konya Graben

1. Introduction
Recent exploration by the Turkish General Directorate of Mineral Research and Exploration (MTA) proved several coal deposits hosted in Neogene sedimentary basins across the country. The most significant one due to its total geological reserves (around 1.8 Gt) is the Karapınar–Ayrancı coal deposit located at the southernmost of Central Turkey; the coal is planned to be exploited and used for feeding the thermal power plant to be installed nearby.

During the late Cenozoic, regional tectonic movements caused the development of fault-controlled basins and volcanic activity in Central Turkey (Toprak and Göncüoğlu, 1993; Dirik and Göncüoğlu, 1996; Bozkurt, 2001; Özsayın et al., 2013; Schildgen et al., 2014). The basin infillings are mainly composed of terrestrial and lacustrine sediments, as well as volcanic and volcanoclastic rocks. The Konya Basin formed during this period of time, occupies almost the entire south Central Turkey. In the southern part of the Konya Basin the Karapınar–Ayrancı coal deposit is

hosted (Figure 1a). Previous studies mostly focused on the regional geological setting and the volcanic rocks at the northern margins of the Konya Basin (Keller, 1974; Ercan et al., 1992; Göncüoğlu and Toprak, 1992; Ulu et al., 1994; Olanca, 1999, Roberts et al., 1999; Gençalioğlu-Kuşçu and Geneli, 2011; Temiz and Savaş, 2014). Coal beds around Karapınar Town have been reported since late 1960s (Gökmen et al., 1993); however, limited number of studies have been conducted about coal quality, geochemical composition and palaeontological findings from central and eastern parts of the deposit after the exploration period of time (Salman and Akyıldız, 2013; Oikonomou, 2015; Redoumi et al., 2016; Altunsoy et al., 2016), whereas only one study (Oskay et al., 2016) dealt with coal petrography and the palaeoenvironmental reconstruction of the coal beds in the eastern part of the deposit. The main objective of the present study was to determine the coal features and to assess the environmental conditions during peat accumulation of the coal seam drilled in the northern part

260

of the Karapınar–Ayrancı coal deposit by the means of petrographic, mineralogical, and geochemical data.

2. Geological setting

The basement and the southern margin of the basin are composed of pre-Neogene rocks (mainly Jurassic to Cretaceous marine limestone), whereas the northern margins consist of Neogene volcanics (Karacadağ volcanics) and the Late Miocene İnsuyu Formation (Figure 1c). The southern part of Central Anatolia began uplifting during Middle to Late Miocene as a result of slab dynamic (Aydar et al., 2013; Schildgen et al., 2014; Gürbüz and Kazancı, 2015), which created accommodation space for the basin infillings in South Central Anatolia and the study area as well (Özsayın et al., 2013; Oskay et al., 2016). These commenced with Late

Miocene fluvial (conglomerate, sandstone and siltstone) and lacustrine sediments (carbonates and claystone). With the onset of Pliocene stronger uplifting in south Central Turkey (Schildgen et al., 2014) resulted in additional relative subsidence; therefore, the coal-bearing Plio-Pleistocene sequence conformably overlies the Late Miocene sedimentary rocks (Figure 1d). This sequence mainly includes fluvial and lacustrine sediments with coal layers. The ostracod and gastropod fauna contained in the inorganic intercalations in the eastern part of the deposit points to peat accumulation during latest Pliocene to Early Pleistocene under freshwater conditions (Redoumi et al., 2016). The floor and roof rocks of the coal seam in the northern part comprise claystone and organic mudstone, whereas claystone, sandstone, and marl are common intercalations within the seam. The coal-bearing sequence
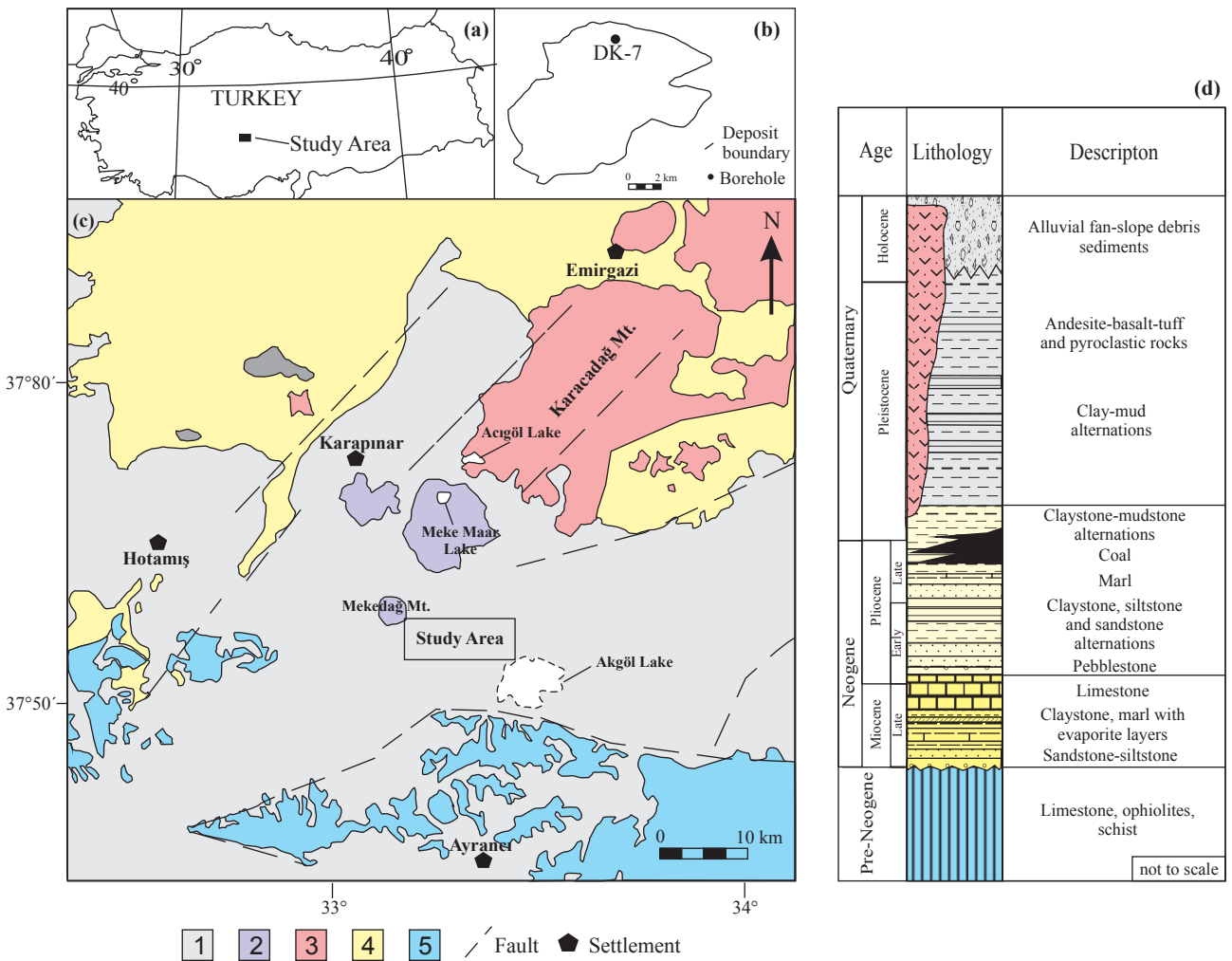

Figure 1. (a) Location map; (b) Schematic map of the Karapınar–Ayrancı coal deposit with borehole location; (c) Geological map of the Karapınar–Ayrancı Basin (modified from Oskay et al., 2016); (d) Stratigraphic column of the Karapınar–Ayrancı Basin (modified and simplified from Oskay et al., 2016, and the references therein). 1: Quaternary sediments, 2: Karapınar Volcanics (Pleistocene), 3: Karacadağ Volcanics (Miocene-Pliocene), 4: İnsuyu Formation (Miocene), 5: Pre-Neogene basement (mostly Mesozoic carbonates).

is overlain by the early Holocene lacustrine sediments and volcanoclastic and volcanic rocks (Dirik and Göncüoğlu, 1996; Olanca, 1999; Karakaya et al., 2004).

3. Material and methods

A total of 26 coal and 20 inorganic sediment samples were picked up from DK-7 core drilled by MTA in the northern part of the Karapınar–Ayrancı coal deposit (Figure 1b). The samples were picked up at depths between 132 and 152 m beneath the current surface; apart from the main seam, there are <0.4-m-thick mineral-rich coal layers above and beneath the coal seam, which were not sampled. The coal lithotypes were identified according to the nomenclature proposed by the International Committee for Coal and Organic Petrology (ICCP, 1993). The routine proximate and ultimate analyses of the coal samples were conducted according to ASTM standards (ASTM D3174, 2004; D3175, 2004; D3302, 2004; D5373, 2004). The gross calorific values of coal samples were determined using an IKA 4000 adiabatic calorimeter (ASTM D5865, 2004). For the coal petrography analysis, polished blocks were prepared from selected coal samples following the ISO 7404-2 (2009) standard and examined using a LEICA DMRX coal-petrography microscope. The maceral nomenclature was based on the ICCP System 1994 (ICCP 2001; Sýkorová et al., 2005; Pickel et al., 2017). The random huminite reflectance was measured on ulminite B according to ISO 7404-5 (2009) standard. The mineralogical composition of the selected bulk coal and inorganic samples was determined using an X-ray Bruker D8 Advance diffractometer equipped with a Lynx-Eye° detector. The scanning area covered the 2θ interval between 4° and 70°, with a scanning angle step of 0.015° and a time step of 1 s. The semiquantitative determination was performed using the Rietveld-based TOPAS® software and applying the technique described in detail by Siavalas et al. (2009). Furthermore, selected polished coal blocks were coated with carbon in order to enlighten the mineralogical composition by means of a JEOL JSM 6300 Scanning Electron Microscope equipped with EDS X-ray analyzer at the Laboratory of Electron Microscopy and Microanalysis, Faculty of Natural Sciences, University of Patras.

4. Results

4.1. Lithological features

In the studied core (Figure 2), the total thickness of the coal seam reaches 20 m with a net cumulative coal thickness of 6.6 m. The coal samples are macroscopically dark in color, matt and brittle, and at sites contain gastropod mollusc shells and clay bands. Carbonate cleat infillings were observed in one sample (DK7/3) only. The coal displays matrix and mineral-rich lithotypes. The matrix lithotype

is commonly weakly gelified and nonstratified. The seam floor consists of claystone and the roof of mudstone. Several inorganic intercalations, which consist of organic-rich mudstone and claystone layers, display variable thickness (Figure 2). Mollusc shell remains (e.g. *Valvata* sp., *Pisidium* sp.) were commonly traced in the intercalations, particularly in mudstone layers; carbonized plant remains were also identified in claystone. The frequent changes between matrix and mineral-rich lithotypes along with several thick gastropod-bearing intercalations indicate changes between limnic and telmatic conditions during peat accumulation; the latter was ceased several times in favor of organic-rich mudstone deposition.

4.2. Coal features

Total moisture ranges from 24.3% to 66.4% (average 44.7%, on as-received basis) and ash yield from 15.9% to 62.3% (average 38.7%, on dry basis); of course, the samples with >50% ash yield are carbonaceous rocks, although they macroscopically were logged as coal. The fossil remains hosted in coal result in an increase of volatile matter yields; thus, ash (up to 62.3%, on dry basis) and volatile matter yields (up to 47.4%, on dry basis) are high due to breakdown of carbonate minerals (Table 1). The calorific values are generally low varying between 7.7 and 21.7 MJ/kg (average 11.4 MJ/kg, on moist, ash-free basis). The ultimate analysis shows that the coal samples are characterized by high total sulfur (up to 8.6%, on dry basis) and hydrogen (up to 9.2 %, on dry basis) contents (Table 1). High total sulfur and hydrogen contents were also reported from central and eastern parts of the deposit (Salman and Akyıldız, 2013; Oskay et al., 2016).

4.3. Maceral composition and huminite reflectance

Table 2 presents the results of the coal-petrography examination. Huminite is the dominant maceral group with telohuminite being the most common subgroup (Figure 3a). In the telohuminite group ulminite predominates (up to 52.0 vol.%, on mineral-free basis); it appears well gelified and ulminite A is common (Figures 3b,c). Furthermore, the presence of telohuminite A could also elevate H contents resulting in positive correlation (r = 0.64) between huminite and H content of the studied samples. Cell lumens of textinite are generally filled in with fluorinite-type resinite (Figure 3d) and corpohuminite, and rarely with mineral matter (e.g., amorphous silica). Densinite (up to 47.5 vol.%) is the common maceral in the detrohuminite group with attrinite contents being generally low (<10.0 vol.%). Detrohuminite macerals are mostly associated with sporinite, liptodetrinite, and mineral matter (e.g., clay minerals and pyrite). Inertinite generally shows low content with fusinite and inertodetrinite being common (Table 2). One distinct feature of the analyzed samples is the relatively high total liptinite content (up to 15.3 vol.%). Liptodetrinite (up to 7.7 vol.%) and resinite, particularly of
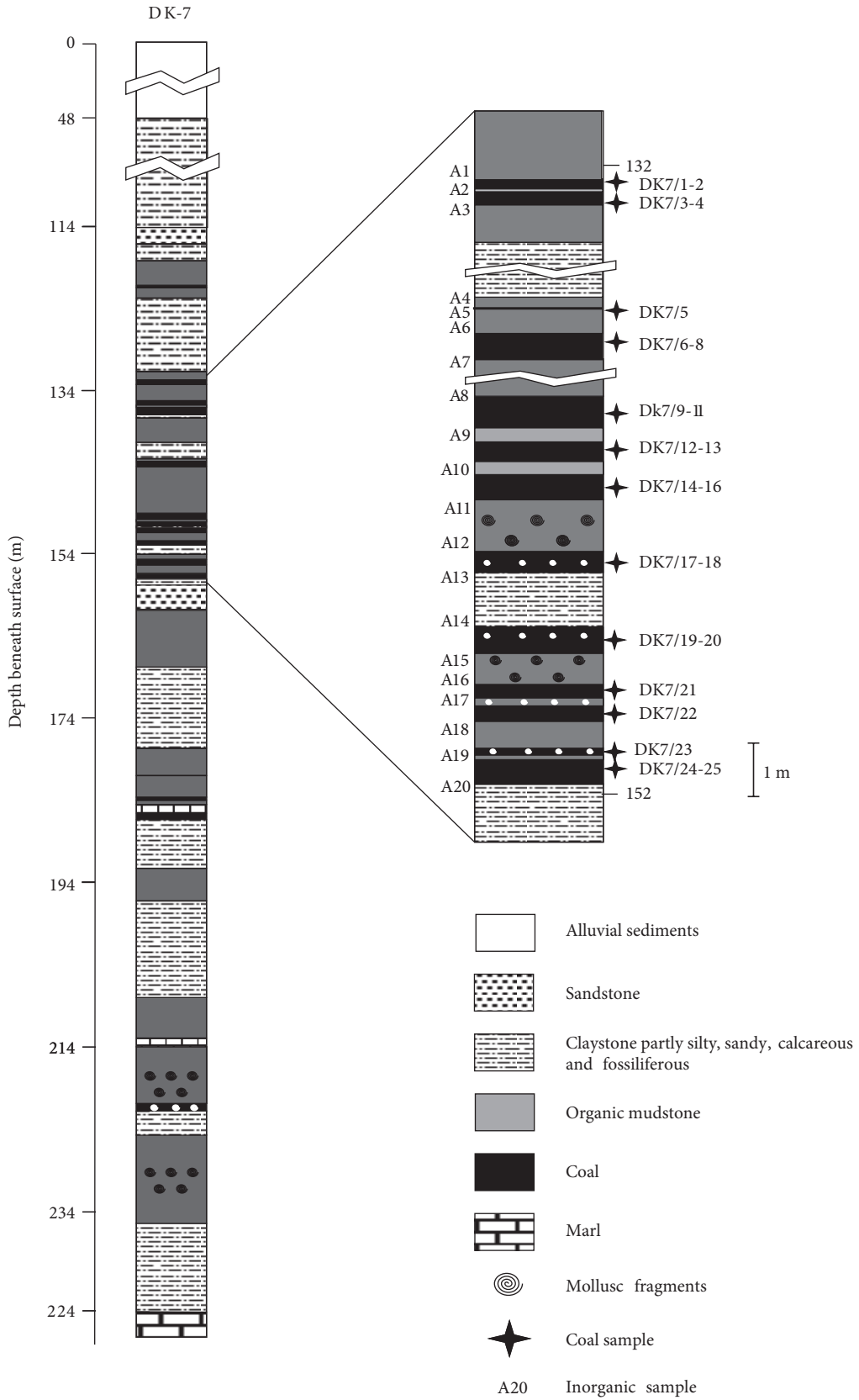
Figure 2. Lithological column of core DK-7 sampled in this study.

Table 1. The results of proximate and ultimate analyses of coal samples from DK-7 borehole in Karapınar-Ayrancı deposit (VM: volatile matter yield; CV: calorific value; ar: as-received basis; db: dry basis; maf: moist, ash-free basis; oxygen content is calculated by subtraction [O = 100 − (C + H + S + N + ash)], in wt.%, db; nd: not determined)

Sample	Total Moisture ar,%	Ash wt.%, db	VM wt.%, db	C	H	N	S	O	CV MJ/kg, maf
				wt.%, db					
DK-7/1	44.1	17.6	37.4	47.9	5.2	1.5	8.3	19.5	11.6
DK-7/2	44.0	16.9	37.6	47.9	5.7	1.7	8.6	19.2	12.0
DK-7/3	46.9	55.1	nd	nd	nd	nd	nd	nd	nd
DK-7/4	44.3	16.7	42.1	48.3	5.3	1.3	8	20.4	11.2
DK-7/5	47.0	54.0	nd	23.4	4.1	0.5	2.3	15.7	nd
DK-7/6	43.4	44.0	35.3	nd	nd	nd	nd	nd	8.5
DK-7/7	51.4	47.6	32.0	27.8	3	0.7	3.7	17.2	9.1
DK-7/8	66.4	51.4	24.4	nd	nd	nd	nd	nd	nd
DK-7/9	42.6	40.7	17.3	32.1	2.1	1	7.1	17	9.6
DK-7/10	49.4	34.0	nd	37	4.6	1.2	6.8	16.4	11.2
DK-7/11	49.2	35.4	nd	nd	nd	nd	nd	nd	10.9
DK-7/12	34.3	62.0	nd	nd	nd	nd	nd	nd	nd
DK-7/13	41.4	22.1	36.6	47.1	5.6	1	7.2	17	12.1
DK-7/14	24.3	15.9	35.9	48.8	5.2	1.4	8.4	20.3	21.7
DK-7/15	52.5	28.1	34.0	44.4	4.9	1.7	7.6	13.3	10.6
DK-7/16	47.0	54.2	nd	nd	nd	nd	nd	nd	nd
DK-7/17	44.5	62.3	28.1	20.7	2.8	0.9	3.1	10.2	7.7
DK-7/18	52.5	35.9	32.8	nd	nd	nd	nd	nd	11.4
DK-7/19	49.3	35.0	nd	nd	nd	nd	nd	nd	10.2
DK-7/20	43.7	28.5	30.1	42.7	9.2	1.4	6.8	11.4	11.0
DK-7/21	44.3	55.5	nd	nd	nd	nd	nd	nd	11.3
DK-7/22	30.7	21.5	47.4	46.7	5.5	1.6	8.4	16.3	15.4
DK-7/23	33.3	61.5	nd	nd	nd	nd	nd	nd	nd
DK-7/24	46.7	33.6	38.0	41.2	4.7	1.4	7.3	11.8	11.1
DK-7/25	43.5	37.5	33.2	37.6	4.6	1.4	6.4	12.5	10.8
Mean	44.7	38.7	33.9	39.6	4.8	1.2	6.7	15.9	11.4

fluorinite type (up to 5.3 vol.%), are common within this maceral group. Mineral matter contents strongly vary (2.0–29.1 vol.%, on whole basis). The minerals identified under the coal-petrography microscope are mostly quartz, clay minerals, pyrite and carbonates (syngenetic and clastic). Furthermore, calcareous fossil shell remains along with siliceous skeletal (diatom) fossil fragments are also traced in the studied samples. In comparison with the maceral composition of the coal from the eastern part (Oskay et al., 2016), the examined samples display relatively higher telohuminite contents, particularly textinite, presumably due to more frequent arboreal peat-forming species thriving on the palaeomire surface.

Huminite reflectance was measured on a limited number of samples only due to the predominance of ulminite A (Table 2). The %Rr values vary between 0.23% and 0.24%. Similar low %Rr values were also reported from the eastern part of the deposit (Oskay et al., 2016). These low values are either related to the existence of H-rich compounds in telohuminite macerals (e.g., resin and wax) and/or low-coalification degree of the analyzed samples (Stout and Spackman, 1989; Suárez-Ruiz et al., 1994; Bechtel et al., 2015; Karayiğit et al., 2016, 2017a; Çelik et al., 2017). The presence of H-rich compounds could suppress %Rr values not corresponding to real coalification degree; therefore, calorific values, moisture and ash yield could be more accurate in rank and grade determination (O'Keefe et al., 2013). Even though moisture is generally higher than 40% (lignite), these values might not be equivalent to bed moisture due to loss of water during transport

Table 2. Maceral composition, huminite random reflectance, and calculated coal indices of the samples from DK-7 borehole in the Karapınar–Ayrancı deposit.

| Sample / Maceral	DK-7/1	-7/2	-7/4	-7/6	-7/9	-7/13	-7/14	-7/15	-7/17	-7/18	-7/20	-7/22	-7/25
vol.% (on mineral matter free basis)													
Textinite	21.4	15.6	15.6	4.7	3.6	17.1	19.1	4.1	1.1	5.5	6.3	10.5	13.5
Ulminite	39.7	45.4	52.0	26.4	30.3	36.8	42.6	31.9	11.8	40.3	30.6	45.7	30.2
Telohuminite	61.1	61.0	67.6	31.1	33.9	53.9	61.7	36.0	12.9	45.8	36.9	56.2	43.7
Attrinite	3.0	0.7	-	36.7	0.4	2.9	-	9.6	25.4	3.8	6.5	1.9	7.4
Densinite	16.0	20.9	13.6	2.8	47.4	26.2	16.3	28.8	34.3	33.6	42.2	26.1	27.8
Detrohuminite	19.0	21.6	13.6	39.5	47.8	29.1	16.3	38.4	59.7	37.4	48.7	28.0	35.2
Gelinite	5.9	0.9	2.2	7.5	0.5	2.4	5.9	5.0	6.9	5.8	1.7	3.1	0.6
Corpohuminite	0.2	1.5	2.2	0.4	1.0	2.6	3.0	0.2	-	1.6	1.5	1.0	1.3
Gelohuminite	6.1	2.4	4.4	7.9	1.5	5.0	8.9	5.2	6.9	7.4	3.2	4.1	1.9
Huminite	86.2	85.0	85.6	78.5	83.2	88.0	87.0	79.6	79.5	90.6	88.8	88.4	80.9
Fusinite	2.2	2.2	1.8	5.1	3.4	0.2	1.0	1.3	1.1	0.4	1.7	1.0	1.0
Inertodetrinite	2.8	2.7	2.2	6.6	3.2	-	0.6	4.3	4.1	1.5	2.2	1.3	3.1
Funginite	-	0.6	-	-	-	-	0.2	-	-	-	-	0.2	-
Semifusinite	0.6	0.4	1.4	2.3	0.6	0.8	0.2	-	-	0.2	1.5	0.5	0.3
Inertinite	5.6	5.7	5.4	14.0	7.2	1.0	1.9	5.6	5.2	2.1	5.4	3.0	4.4
Sporinite	1.1	0.6	1.4	1.1	0.6	0.4	1.7	1.8	6.6	1.6	1.0	2.3	1.7
Cutinite	1.7	0.4	1.8	0.2	-	2.4	3.0	0.6	0.2	-	0.3	0.6	0.9
Suberinite	0.2	0.2	-	-	-	0.7	-	0.4	-	0.2	-	0.2	0.2
Alginite	-	0.2	-	-	0.2	0.2	0.2	0.2	-	-	0.2	0.2	0.2
Liptodetrinite	3.2	3.5	1.4	6.2	6.2	4.4	1.5	6.8	7.7	2.4	3.7	2.4	6.4
Resinite	0.4	1.5	0.5	-	-	0.2	1.9	0.9	0.2	1.3	0.3	0.9	-
Fluorinite	1.6	2.9	3.9	-	2.6	2.8	2.8	4.1	0.6	1.8	0.3	2.0	5.3
Liptinite	8.2	9.3	9.0	7.5	9.6	11.0	11.1	14.8	15.3	7.3	5.8	8.6	14.7
vol.% (on whole sample)													
Mineral matter	3.2	4.0	2.3	29.1	4.3	4.9	4.8	4.8	25.3	13.8	9.1	2.0	7.2
Mean Rr_o (%)			0.23			0.23	0.24					0.24	
Standard Dev. (±)			0.02			0.02	0.02					0.03	
PetrographicIndices (dimensionless)													
GI	2.1	3.1	3.3	0.7	7.1	3.2	3.2	3.4	1.7	7.2	4.2	4.9	2.4
TPI	2.3	2.6	4.0	0.7	0.7	1.8	2.9	0.8	0.2	1.1	0.8	1.8	1.2
GWI	0.4	0.4	0.3	0.8	1.6	0.6	0.5	0.9	2.0	1.2	1.3	0.6	0.7
VI	2.8	2.5	4.6	0.8	0.7	1.8	3.9	0.9	0.3	1.2	0.8	2.0	1.2
A	66.3	68.1	77.4	32.8	38.1	62.9	74.2	44.0	20.5	52.3	40.3	63.3	53.2
B	28.1	26.2	17.2	53.2	54.7	36.1	23.9	50.4	74.3	45.6	54.3	33.7	42.4
C	5.6	5.7	5.4	14.0	7.2	0.9	1.9	5.6	5.2	2.1	5.4	3.0	4.4
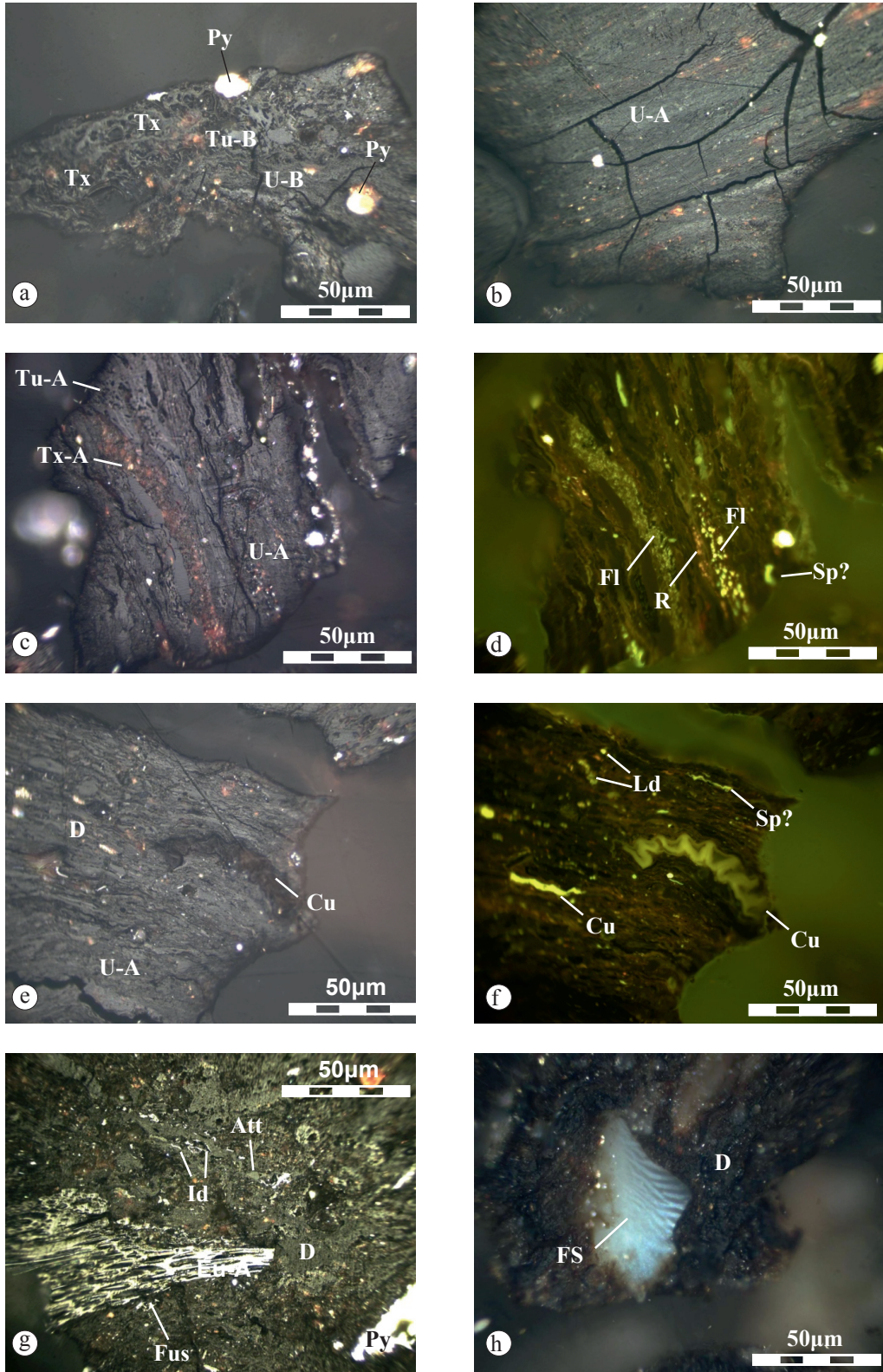
Figure 3. Photomicrographs of coal samples from DK-7 core: textinite (T), textinite A (T-A), ulminite A (U-A), ulminite B (U-B), densinite (D), attrinite (A), resinite (R), fluorinite-type resinite (Fl), cutinite (Cu), sporinite (Sp), fusinite (Fus), liptodetrinite (Ld), pyrite (Py) and mollusc fossil remain (FS). All photomicrographs were taken under incident white light (a, b, c, e, g, h) and blue-light excitation (d and f), oil immersion, 500× total magnification.

from sampling site to laboratory. Considering calorific values and ash yields of the studied samples, the studied samples are low- to very-low-grade, low-rank C to A coal and moderately high- to high-ash low-rank C (lignite) according to ECE-UN (1998) and ISO-11760 (2005) classifications, respectively. Furthermore, samples with high ash yield (≥50%, db) due to the presence of fossil shell remains and clay bands are considered carbonaceous rocks.

4.4. Mineralogical composition

4.4.1 Minerals in coal

The silicate minerals are the dominant phases, whereas carbonates, particularly calcite, are dominant in the shell-bearing samples (Table 3). Pyrite and sulfate minerals are generally minor phases. The XRD data is certified through the SEM-EDX results and additionally, some accessory minerals, such as apatite, barite, chromite, dolomite, monazite, titanite, and Ti-oxides, were identified.

The predominance of silicate minerals along with the high ash yields imply that the clastic input was high during peat accumulation; this is also supported by both petrographical and SEM findings. The clay minerals are mostly aggregated with other clastic minerals (e.g., quartz, feldspars) and attrinite as well. In fossil shell-bearing coals, aragonite is commonly identified; however, in the studied core this is traced in one coal sample (DK7/5) only. The lack of aragonite here, as well as its low content commonly reported from fossil shell-bearing, low-rank coals in Turkey (Demirel and Karayiğit, 1999; Querol et al., 1999; Karayiğit et al., 2000, 2015, 2017b), might be due to transformation of aragonite into calcite during coalification

Table 3. Rietveld-based XRD quantification results of coal samples from the DK-7 borehole, in wt.% of the crystalline phase (CM: clay minerals; Gyps/Bas: gypsum/bassanite; +++ = dominant phase > 35 wt%, ++ = abundant phase 35–5 wt%, += minor phase < 5 wt %).

Sample \ Mineral	Quartz	Calcite	Aragonite	CM	Mica	Feldspar	Pyrite	Gyps/Bas
DK-7/1	+++				++	++	++	
DK-7/2	+++					+++		++
DK-7/3	+++	+				++		
DK-7/4	+++	++				++		
DK-7/5	+	+++	+					
DK-7/6	+	+++						
DK-7/7	+	+++						
DK-7/8	+	+++					+	
DK-7/9	+++				+++	++	+	
DK-7/10	+++				++	++		
DK-7/11	+			+++		++		
DK-7/12	+++							++
DK-7/13	+++							++
DK-7/14	+++			++		++	+	+
DK-7/15	++	+		+++			+	
DK-7/16	++			+++		+		+
DK-7/17	++			+++		++		+
DK-7/18	+++	+			++	++	++	++
DK-7/19	+++				++	++		
DK-7/20	++	+++		++		++		
DK-7/21	+++				+++	++		++
DK-7/22	++	+			+++	++	+	
DK-7/23	++			+++	++			
DK-7/24	+++				++	++	++	
DK-7/25	+++					+++		++

(Ward, 2002). Framboidal pyrite crystals are common in the studied samples, whereas massive pyrite crystals are barely identified. Pyrite crystals appear in the form of framboidal crystals and less commonly as individual crystals within ulminite. Framboidal pyrite crystals are generally syngenetic and related with reducing conditions within the palaeomire (Kostova et al., 2005; Chou, 2012). The surface runoff from the Neogene volcanic rocks, as well as the lacustrine carbonates in the northern margins were presumably the sources of detrital minerals (e.g. clay minerals, quartz, feldspar); nevertheless, the occurrence of syngenetic framboidal pyrite crystals and silica filling in shell remains and maceral cell-lumens/cavities indicates that authigenic precipitation took place during a time period of low clastic input. Furthermore, mica and feldspar possibly derived from volcanic rocks on the margins, could easily convert to chlorite and/or kaolinite within the palaeomire (Kostova and Zdravkov 2007; Dai and Chou, 2007; Dai et al., 2008, 2017); therefore, clay minerals might also be considered alteration products of mica and feldspars.

Bassanite is mostly reported in low-temperature ash of coal (Ward, 2002); however, the cooccurrence with gypsum in some coal samples suggests that bassanite is formed through dehydration of gypsum during storage and/or

transportation from the sampling site (Siavalas et al., 2009; Koukouzas et al., 2010; Ward, 2016). The mineralogical composition of the studied samples is similar to that of the samples obtained from the eastern part of the Karapınar–Ayrancı coal deposit (Oskay et al., 2016); in contrast, halite is lacking in the examined samples. This is presumably related to the chemistry of circulating solutions; in this part of the deposit, salinity seems to have been low. Thus, halite could not epigenetically precipitate. In addition, carbonates filling in cleats in one sample (DK7/3) could imply that the epigenetic solutions were Ca-rich and maybe originated from intraseam leaching.

4.4.2 Minerals in inorganic sediments

The mineralogical composition of the inorganic intercalations slightly differs from this of coal (Table 4). Carbonates, particularly calcite, along with clay minerals are dominant phases. Calcite displays higher concentrations in shell-bearing samples, in which aragonite is also determined. Beside clay minerals, silicates are generally minor phases probably due to masking effect through the abundant shell remains. Cristobalite, pyrite and gypsum are determined in few inorganic samples and dolomite in one intercalation sample (A17) only. The common occurrence of shell remains within the organic mudstone could imply the discharge of Ca-rich waters into

Table 4. Rietveld-based XRD quantification results of the inorganic sediment samples from the DK-7 borehole, in wt.% of the crystalline phase (Cris: cristobalite, CM: clay minerals; +++ = dominant phase > 35 wt%, ++ = abundant phase 35–5 wt%, += minor phase < 5 wt %).

Mineral / Sample	Quartz	Cris	Calcite	Aragonite	Dolomite	CM	Mica	Feldspar	Pyrite	Gypsum
A1	+		++							
A2	++	+	+++				++		+	
A3	++	+	+			+++		+		
A4	+		+++	+					+	
A5			+++	++		+			+	
A6	+		+++	+		++				
A7	+		+++	++						
A9	++		++			+++		++		
A11	+		+++						+	
A12	++		+			+++			+	
A13	+++		++				++	++	+	+
A14	++		++			+++		+	+	
A15	++	+	+++			+++		++		
A16	++		+++	+		++		+		
A17	+		+++	+	+		++		++	
A19	+		+++	+						
A20	+		+++					+		++

the palaeomire/palaeolake along with elevated water table. Consequently, peat accumulation was ceased several times in the studied part of the basin. These conditions might have allowed the development of alkaline conditions, under which the preservation of organic matter is low (Mendonça Filho et al., 2010; Karayiğit et al., 2017b).

5. Discussion

Several facies diagrams and indices contributing to palaeoenvironmental mire reconstruction have been introduced by several researchers (Calder et al., 1991; Diessel, 1992; Singh and Singh, 2000; Petersen and Ratanasthein, 2011) and still some objections have been raised concerning the accuracy of these diagrams (Crosdale, 1993; Dehmer, 1995; Wüst et al., 2001; Scott, 2002; Moore and Shearer, 2003). Nevertheless, the coal diagrams and indices, along with mineralogical, geochemical, sedimentological, and palaeontological data, might be useful for approaching the palaeoenvironmental conditions (e.g., hydrological and water chemistry) and the dominant vegetation in the palaeomire (Kalaitzidis et al., 2004; Zdravkov et al., 2011; Bechtel et al., 2015; Karayiğit et al., 2016, 2017b; Çelik et al., 2017).

The coal-petrography data plotted on the Mukhopadhyay's ternary diagram implies mixed vegetation on the palaeomire's surface with arborescent plants being occasionally dominant (Figure 4). These samples contain relatively higher amounts of telohuminite and fluorinite pointing to small trees and shrubs (e.g. Myricaceae) on palaeomire's surface (O'Keefe et al., 2013; Pickel et al., 2017). Lack of xylite-rich lithotype leads to the conclusion that the contribution of the arboreal vegetation, mostly represented by small trees and shrubs, was moderate but definitely no forested mire was established during peat accumulation in the northern part of the deposit. Besides, the abundance of detrohuminite mixed up with liptodetrinite in some samples indicates significant contribution of reed/sedge vegetation. Appropriate pH and water-level conditions can be another explanation for the good preservation of cell structure. Almost all samples are projected on the lowest part of the Mukhopadhyay's diagram indicating relatively strong anoxic conditions in the northern part of the deposit in comparison to the eastern one; this suggests rather high and relatively stable watertable in the palaeomire during peat accumulation (Oskay et al., 2016). One sample (DK-7/6) projected on slightly oxic conditions is related to the associations between inertodetrinite and detrohuminite macerals (Figure 3g; Table 2). This association points to the allochthonous origin of inertinite macerals and the water-logged mire surface (Diessel et al., 2010; Silva et al., 2008; O'Keefe et al., 2013).
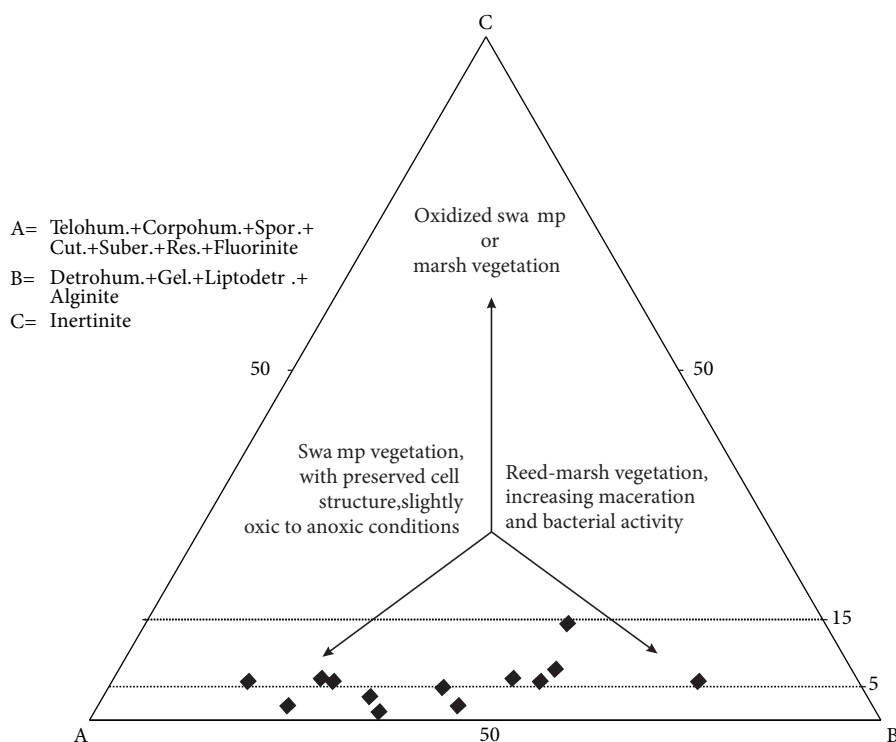

Figure 4. ABC ternary plot of analyzed coal samples from DK-7 core (after Mukhopadhyay, 1989).

The tissue preservation index (TPI) vs. gelification index (GI) diagram along with the vegetation index (VI) vs. groundwater influence (GWI) diagram are also applied in an attempt to reconstruct the conditions during peat accumulation in the northern part of the basin (Figures 5a and 5b). Of note, all these indices were calculated according to modifications introduced by Kalkreuth et al. (1991) and Kalaitzidis et al. (2004) for Tertiary low-rank coals. The TPI values range between 0.2 and 4.0 suggesting moderate organic matter preservation. TPI values are relatively high (>1; see Table 2) in the upper part of the seam. As previously explained, high telohuminite contents are presumably related to trees and/or shrubs/bushes on the mire surface. The GI values vary from 0.7 to 7.2 and only one sample displays GI < 1 (Figure 5a). The GI values suggest that organic matter in this part of the deposit is, in general, gelified under relatively higher and stronger fluctuating water level during peat accumulation than in the eastern part (Oskay et al., 2016). The VI values range between 0.3 and 4.6 (Table 2, Figure 5b). The highest VI values are generally recorded in the upper part of the seam and suggest that preservation of vegetal tissues developed under relatively more acidic and reducing conditions; however, VI values < 1.0 indicate occasional dominance of herbaceous vegetation in the palaeomire (Kalaitzidis et al., 2004; Silva et al., 2008; Siavalas et al., 2009; Karayiğit et al., 2016). The GWI values vary from 0.3 to 2.0 which may suggest that the peat accumulation of the studied part of the deposit commenced under mesotrophic hydrological regime and turned into the alternations of mesotrophic and rheotrophic (GWI > 1) conditions. Finally, the upper part of the coal seam was accumulated under ombrotrophic (GWI < 0.5) condition; this suggests that rainfall became more important for the continuation of peat accumulation in the mire. The GI values of these samples are generally slightly high indicating wet conditions; nevertheless, these GWI values could be either the indicator of forested mire or a masking effect of high telohuminite contents (Koukouzas et al., 2010; Oikonomopoulos et al., 2015; Mitrovic et al., 2016; Karayiğit et al., 2017b; Çelik et al., 2017). The latter seems to fit better due to the lack of xylite-rich lithotype and the abundance of fluorinite-type resinite within textinite.

The coal facies diagrams show that the water table was high enough to maintain the wetness of the accumulated peat in the palaeomire resulting in anoxic conditions. Under such conditions, the commonly encountered syngenetic framboidal pyrite crystals can easily form (Chou, 2012; Oikonomopoulos et al., 2015). This crystal morphology can also be an indicator of the formation of slightly acidic to neutral conditions in the palaeomire (Querol et al., 1989). This could be related with sulfate-rich water supply into palaeomire resulting in well tissue

preservation and high total S contents (Kostova et al., 2005; Siavalas et al., 2009, Karayiğit et al., 2015). The shell-bearing coal beds along with the syngenetic carbonates are related to alkaline conditions within the palaeomire (Querol et al., 1996; Siavalas et al., 2009; Karayiğit et al., 2017b). The coexistence of carbonate minerals and syngenetic pyrite implies rather the development of neutral conditions and the influence of calcium- and sulphate-rich water supply into the palaeomire. The shell remains also support the elevated water table shifting the telmatic to limnotelmatic conditions. In turn, herbaceous vegetation, particularly reed plants, was more common on the palaeomire surface, and the detrohuminite and liptodetrinite contents increased. The elevated water table also resulted in the deposition of the shell-bearing organic matter and peat accumulation was ceased several times in favor of lacustrine conditions. The predominance of carbonate minerals in the intercalations could be explained by the common occurrence of fossil remains rather than by increased Ca concentrations in the water of the palaeolake. Moreover, the variations on ash yield and the occurrence of clay-bearing coal reflects the influence of sediment laden from marginal areas, presumably related to high runoff from margins during peat accumulation and/or increased fluvial impact for short periods of time. Due to the dominance of silicate minerals the clastic material seems deriving from volcanic rocks outcropping at the northern margins. Considering the lack of Mesozoic carbonates at the northern margins (Figure 1), the leached surface waters from the volcanic rocks rather than the karstic water could also supply sulfur as in the eastern part of the basin (Oskay et al., 2016). Overall, peat was accumulating under pure telmatic to limnotelmatic conditions, whereas elevated water table and fluvial contribution ceased peat accumulation several times. Even though the results of this study are based on samples obtained from one drilling site only located in the northern part of the deposit, the vegetation seems to be relatively different from that dominating in the eastern part. Here, the contribution of woody vegetation might have been slightly higher than in the eastern part; however, the maceral composition denotes that the difference could be caused by the presence of clusters of shrubs/bushes on the palaeomire surface rather than by real dense forests.

6. Conclusion

The tectonic movements during Pliocene to Pleistocene created subsidence, and consequently, accommodation space and favorable lacustrine and telmatic conditions in the northern part of the Karapınar–Ayrancı coal deposit in a similar way to that in the eastern part. Some slight differences were recorded on petrographical and mineralogical compositions between both parts of the
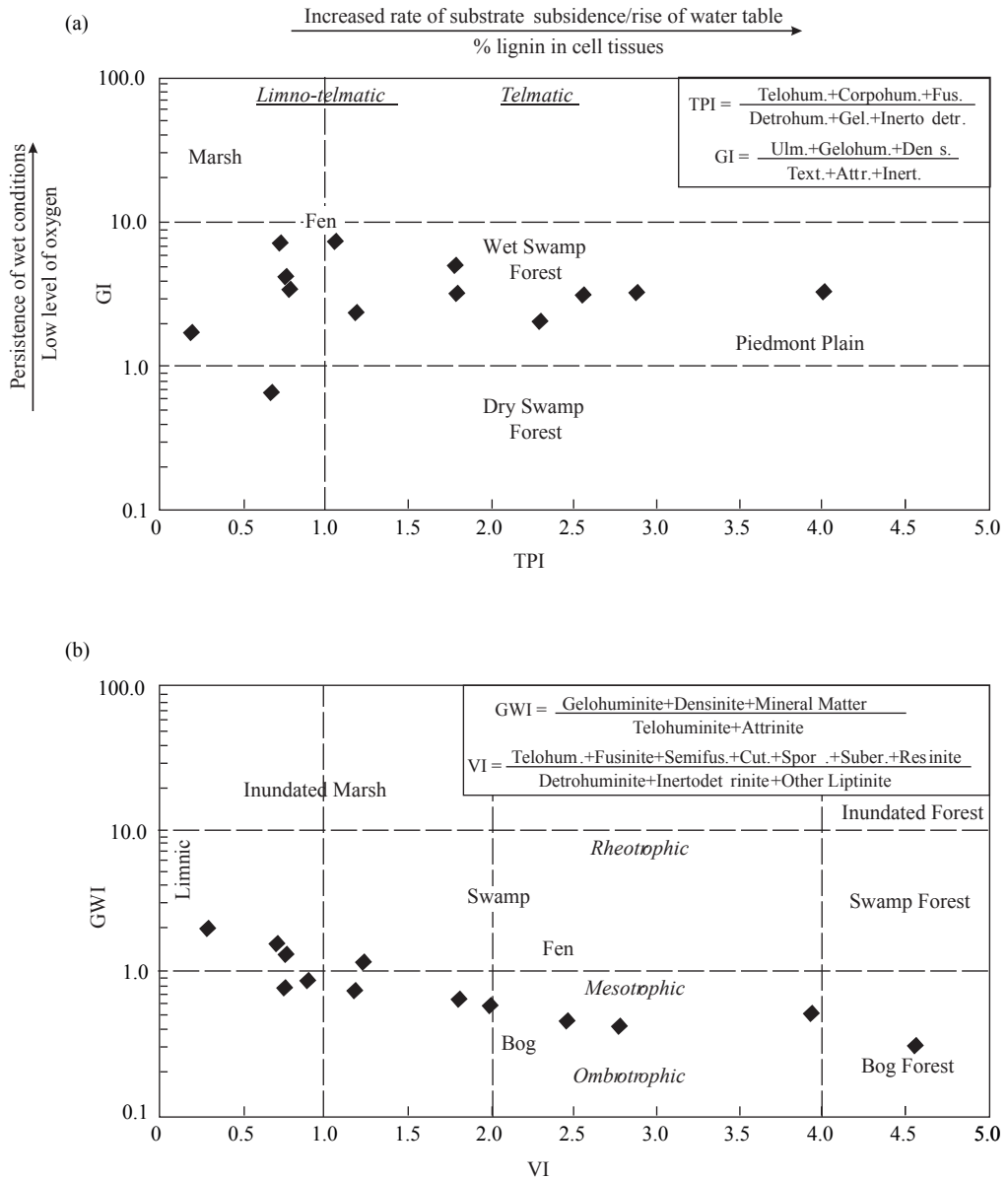
(a)

$$\xrightarrow{\text{Increased rate of substrate subsidence/rise of water table}}$$
% lignin in cell tissues

$$TPI = \frac{Telohum.+Corpohum.+Fus.}{Detrohum.+Gel.+Inerto\ detr.}$$

$$GI = \frac{Ulm.+Gelohum.+Den\ s.}{Text.+Attr.+Inert.}$$

(b)

$$GWI = \frac{Gelohuminite+Densinite+Mineral\ Matter}{Telohuminite+Attrinite}$$

$$VI = \frac{Telohum.+Fusinite+Semifus.+Cut.+Spor.+Suber.+Resinite}{Detrohuminite+Inertodetrinite+Other\ Liptinite}$$

Figure 5. (a) GI vs. TPI plot of the coal samples from DK-7 core (after Diessel, 1992, as modified by Kalaitzidis et al., 2004); (b) VI vs. GWI plot of analyzed coal samples from DK-7 core (after Calder et al., 1991, as modified by Kalaitzidis et al., 2004).

basin. These differences seem to be related with the peat-forming vegetation and the water table. The coal facies along with the mineralogical and the geochemical data imply that peat was accumulating mostly under mesotrophic to rheotrophic, anoxic conditions. Therefore, syngenetic framboidal pyrite is common; its occurrence along with syngenetic carbonates is the evidence for neutral conditions during peat accumulation. Moderate to high TPI and VI values indicate significant contribution of woody vegetation. In contrast, the maceral composition (e.g., fluorinite-type resinite) indicates the presence of

shrubs/bushes on palaeomire's surface. The abundance of shell remains and the varying contents of detrital minerals along the examined seam profile could be related to the fluctuating water level, and in turn, changes in the clastic input from the margins. Thus, coal is generally characterized by high ash yield and low gross calorific value. Water table rise ceased peat accumulation and established lacustrine conditions several times resulting in the formation of inorganic intercalations. Overall, the precursor peat was presumably accumulated under pure telmatic to limnotelmatic conditions and spatial variability

seems to be developed in the palaeomires of the Karapınar–Ayrancı coal deposit.

References

Altunsoy M, Sari A, Özçelik O, Engin H, Hökerek, S (2016). Major and trace-element enrichments in the Karapinar coals (Konya, Turkey). Energ Source Part A 38: 88-99.

American Society for Testing and Materials (ASTM) D3174 (2004). Standard method of ash in the analysis sample of coal and coke from coal. Annual Book of ASTM Standards 2004. Gaseous Fuels: Coal and Coke 05.06. ASTM, Philadelphia, PA, pp. 322-326.

American Society for Testing and Materials (ASTM) D3175 (2004). Standard method of volatile matter in the analysis sample of coal and coke from coal. Annual Book of ASTM Standards 2004. Gaseous Fuels: Coal and Coke 05.06. ASTM, Philadelphia, PA, USA, p. 327-330.

American Society for Testing and Materials (ASTM) D3302 (2004). Standard method of total moisture in coal. Annual Book of ASTM Standards 2004. Gaseous Fuels: Coal and Coke. ASTM, Philadelphia, PA, USA, pp. 352-358.

American Society for Testing and Materials (ASTM) D5373 (2004). Standard test methods for instrumental determination of carbon, hydrogen, and nitrogen in laboratory samples of coal and coke. Annual Book of ASTM Standards 2004.Gaseous Fuels: Coal and Coke. ASTM, Philadelphia, PA, USA, pp. 504-507.

American Society for Testing and Materials (ASTM) D5865 (2004). Standard test method for gross calorific value of coal and coke. Annual Book of ASTM Standards 2004. Gaseous Fuels: Coal and Coke 05.06. ASTM, Philadelphia, PA, USA, pp. 519-529.

Aydar E, Çubukçu HE, Şen E, Akın L (2013). Central Anatolian Plateau, Turkey: incision and paleoaltimetry recorded from volcanic rocks. Turk J Earth Sci 22: 739-746.

Bechtel A, Karayiğit Aİ, Sachsenhofer RF, Inaner H, Christanis K, Gratzer R (2015). Spatial and temporal variability in vegetation and coal facies as reflected by organic petrological and geochemical data in the Middle Miocene Çayirhan coal field (Turkey). Int J Coal Geol 134-135: 46-60.

Bozkurt E (2001). Neotectonics of Turkey - a synthesis. Geodin Acta 14: 3-30.

Calder J, Gibling M, Mukhopadhyay P (1991). Peat formation in a Westphalian B piedmont setting, Cumberland Basin, Nova Scotia. B Soc Geol Fr 162: 283-298.

Çelik Y, Karayiğit Aİ, Querol X, Oskay RG, Mastalerz M, Kayseri Özer MS (2017). Coal characteristics, palynology, and palaeoenvironmental interpretation of the Yeniköy coal of Late Oligocene age in the Thrace Basin (NW Turkey). Int J Coal Geol 181: 103-123.

Chou CL (2012). Sulfur in coals: A review of geochemistry and origins. Int J Coal Geol 100: 1-13.

Crosdale PJ (1993). Coal maceral ratios as indicators of environment of deposition: do they work forombrogenous mires? An example from the Miocene of New Zealand. Org Geochem 20: 797-809.

Dai S, Chou C-L (2007). Occurrence and origin of minerals in a chamosite-bearing coal of Late Permian age, Zhaotong, Yunnan, China. Am Mineral 92: 1253-1261.

Dai S, Tian L, Chou C-L, Zhou Y, Zhang M, Zhao L, Wang J, Yang Z, Cao HZ, Ren D (2008). Mineralogical and compositional characteristics of Late Permian coals from an area of high lung cancer rate in Xuanwei, Yunnan, China: occurrence and origin of quartz and chamosite. Int J Coal Geol 76: 318-327.

Dai S, Xie P, Jia S, Ward CR, Hower HC, Yan X, French D (2017). Enrichment of U-Re-V-Cr-Se and rare earth elements in the Late Permian coals of the Moxinpo Coalfield, Chongqing, China: Genetic implications from geochemical and mineralogical data. Ore Geol Rev 80: 1-17.

Dehmer J (1995). Petrological and organic geochemical investigation of recent peats with known environments of deposition. Int J Coal Geol 28: 111-138.

Demirel İHD, Karayiğit Aİ (1999). Quality and petrographic characteristics of the lacustrine Ermenek coal (early Miocene), Turkey. Energ Source 21: 329-338.

Diessel C, Boyd R, Wadsworth J, Leckie D, Chalmers G (2010). On balanced and unbalanced accommodation/peat accumulation ratios in the Cretaceous coals from Gates Formation, Western Canada, and their sequence-stratigraphic significance. Int J Coal Geol 43: 143-186.

Diessel CFK (1992). Coal-bearing depositional systems. Berlin, Germany: Springer.

Dirik K, Göncüoğlu C (1996). Neotectonic characteristic of central Anatolia. Int Geol Rev 38: 807-817.

Economic Commission for Europe-United Nations (E.C.E.-U.N.), (1998). International Classification of in-seam Coals. Energy/19, Geneva: ECE.

Ercan T, Tokel S, Matsuda JI, Ui T, Notsu K, Fujitani T (1992). New geochemical, isotopic and radiometric data of Quaternary volcanism of Hasandağ-Karacadağ (Central Anatolia). Bull Geol Cong Turkey 7: 8-21.

Gençalioğlu-Kuşçu G, Geneli F (2011). Review of post-collisional volcanism in the Central Anatolian Volcanic Province (Turkey), with special reference to the Tepekoy Volcanic Complex. Int J Earth Sci 100: 1967-1985.

Gökmen V, Memikoğlu O, Dağlı M, Öz D, Tuncalı E (1993). Inventory of Turkish lignites. Ankara: MTA Publication.

Göncüoğlu MC, Toprak, V (1992). Neogene-quaternary volcanism of central Anatolia: a volcanostructural evaluation. Bull Sec Volcanol Soc Géol Fr 27: 1-6.

Gürbüz A, Kazanci N (2015). Genetic framework of Neogene-Quaternary basin closure process in central Turkey. Lithosphere 7: 421-426.

International Committee for Coal and Organic Petrology (ICCP) (1993). International Handbook of Coal Petrography, 3rd suppl. to 2nd ed. Paris, France: Centre National de la Recherche Scientifique.

International Committee for Coal Petrology (ICCP) (2001). The new inertinite classification (ICCP System 1994). Fuel 80: 459-471.

International Organization for Standardization (ISO) 7404-2 (2009). Methods for the petrographic analysis of coals — Part 2: methods of preparing coal samples. Geneva, Switzerland: International Organization for Standardization.

International Organization for Standardization (ISO) 7404-5 (2009). Methods for the petrographic analysis of coal — Part 5: method of determining microscopically the reflectance of vitrinite. Geneva, Switzerland: International Organization for Standardization.

International Organization for Standardization (ISO) 11760 (2005). Classification of coals. Geneva, Switzerland: International Organization for Standardization.

Kalaitzidis S, Bouzinos A, Papazisimou S, Christanis K (2004). A short-term establishment of forest fen habitat during Pliocene lignite formation in the Ptolemais Basin, NW Macedonia, Greece. Int J Coal Geol 57: 243-263.

Kalkreuth WD, Marchioni DL, Calder JH, Lamberson MN, Naylor RD, Paul J (1991). The relationship between coal petrography and depositional environments from selected coal basins in Canada. Int J Coal Geol 19: 21-76.

Karakaya N, Çelik-Karakaya M, Temel A, Küpeli S, Tunoglu C (2004). Mineralogical and chemical characterization of sepiolite occurrences at Karapınar (Konya Basin, Turkey). Clay Clay Miner 52: 495-509.

Karayiğit Aİ, Bircan C, Mastalerz M, Oskay RG, Querol X, Lieberman NR (2017a). Coal characteristics, elemental composition and modes of occurrence of some elements in the İsaalan coal (Balıkesir, NW Turkey). Int J Coal Geol 172: 43-59.

Karayiğit Aİ, Gayer RA, Querol X, Onacak T (2000). Contents of major and trace elements in feed coals from Turkish coal-fired power plants. Int J Coal Geol 44: 169-184.

Karayiğit Aİ, Littke R, Querol X, Jones T, Oskay RG, Christanis K (2017b). The Miocene coal seams in the Soma Basin (W. Turkey): Insights from coal petrography, mineralogy and geochemistry. Int J Coal Geol 173: 110-128.

Karayiğit Aİ, Oskay RG, Christanis K, Tunoğlu C, Tuncer A, Bulut Y (2015). Palaeoenvironmental reconstruction of the Çardak coal seam, SW Turkey. Int J Coal Geol 139: 3-16.

Karayiğit Aİ, Oskay RG, Tuncer A, Mastalerz M, Gümüş BA, Şengüler I, Yaradılmış H, Tunolğu C (2016). A multidisciplinary study of the Gölbaşı-Harmanlı coal seam, SE Turkey. Int J Coal Geol 167: 31-47.

Keller J (1974). Quaternary maar volcanism near Karapınar in central Anatolia. B Volcanol 38: 378-396.

Kostova I, Marinov S, Stefanova M, Markova K, Stamenova V (2005). The distribution of sulphur forms in high-S coals of the Maritza West Basin, Bulgaria. B Geosci 80: 23-32.

Kostova I, Zdravkov A (2007). Organic petrology, mineralogy and depositional environment of the Kipra lignite seam, Maritza-West Basin, Bulgaria. Int J Coal Geol 71: 527-541.

Koukouzas N, Kalaitzidis SP, Ward CR (2010). Organic petrographical, mineralogical and geochemical features of the Achlada and Mavropigi lignite deposits, NW Macedonia, Greece. Int J Coal Geol 83: 387-395.

Mendonça Filho JGM, Chagas RBA, Menezes TR, Mendonça JO, da Silva FS, Sabadini-Santos E (2010). Organic facies of the Oligocene lacustrine system in the CenozoicTaubaté basin, Southern Brazil. Int J Coal Geol 84: 166-178.

Mitrović D, Đoković N, Životić D, Bechtel A, Šajnović A, Stojanović K (2016). Petrographical and organic geochemical study of the Kovin lignite deposit, Serbia. Int J Coal Geol 168: 80-107.

Moore TA, Shearer JC (2003). Peat/coal type and depositional environment: are they related? Int J Coal Geol 56: 232-252.

Mukhopadhyay P (1989). Organic Petrography and Organic Geochemistry of Tertiary Coals from Texas in Relation to Depositional Environment and Hydrocarbon Generation. Report of Investigations, Texas: Bureau of Economic Geology.

Oikonomopoulos IK, Kaouras G, Tougiannidis N, Ricken W, Gurk M, Antoniadis P (2015). The depositional conditions and the palaeoenvironment of the Achlada xylite-dominated lignite in western Makedonia, Greece. Palaeogeogr Palaeoclimatol Palaeoecol 440: 777-792.

Oikonomou K (2015). Potential impact of sulphur, fluorine and chlorine concentrations of lignite Karapınar (Turkey) in future mining operation. MSc, University of Patras, Rio-Patras, Greece (in Greek).

O'Keefe JMK, Bechtel A, Christanis K, Dai S, Di Michele WA, Eble CF, Esterle JS, Mastalerz M, Raymond AL, Valentim BV, Wagner NJ, Ward CR, Hower JC (2013). On the fundamental difference between coal rank and coal type. Int J Coal Geol 118: 58-87.

Olanca K (1999). Quaternary volcanism of Karapınar-Konya region: geochemical evaluation. Yerbilimleri 21: 115-124 (in Turkish with an abstract in English).

Oskay RG, Christanis K, Inaner H, Salman M, Taka M (2016). Palaeoenvironmental reconstruction of the eastern part of the Karapınar-Ayrancı coal deposit (Central Turkey). Int J Coal Geol 163: 100-111.

Özsayın E, Çiner TA, Rojay BF, Dirik KR, Melnick D, Fernández-Blanco D, Bertotti G, Schildgen TF, Garcin Y, Strecker MR, Sudo M (2013). Plio-quaternary extensional tectonics of the central Anatolian plateau: A case study from the Tuzgölü Basin, Turkey. Turk J Earth Sci 22: 691-714.

Petersen HI, Ratanasthien B (2011). Coal facies in a Cenozoicparalic lignite bed, Krabi Basin, southern Thailand: Changing peat-forming conditions related to relative sea-level controlled watertable variations. Int J Coal Geol 87: 2-12.

Pickel W, Kus J, Flores D, Kalaitzidis S, Christanis K, Cardott BJ, Misz-Kennan M, Rodrigues S, Hentschel A, Hamor-Vido M, Crosdale P, Wagner N (2017). Classification of liptinite - ICCP System 1994. Int J Coal Geol 169: 40-61.

Querol X, Cabrera Ll, Pickel W, López-Soler A, Hagemann HW, Fernández-Turiel JL (1996). Geological controls on the coal quality of the Mequinenza subbituminous coal deposit, northeast Spain. Int J Coal Geol 29: 67-91.

Querol X, Chinenon S, López-Soler A (1989). Iron sulphide precipitation sequence in Albian coals from the Maestrazgo basin, southeastern Iberean range, northeastern Spain. Int J Coal Geol 11: 171-189.

Querol X, Alastuey A, Plana F, Lopez-Soler A, Tuncali E, Toprak S, Ocakoglu F, Koker A (1999). Coal geology and coal quality of the Miocene Mugla basin, southwestern Anatolia, Turkey. Int J Coal Geol 41: 311-332.

Redoumi E, Iliopoulos G, Oskay RG, Salman M, Christanis K (2016). Preliminary results from the micropalaeontological study of the Karapınar-Ayrancı coal Deposit (South-Central Anatolia, Turkey). Proceedings of the 17th Paleontology-Stratigraphy Workshop, pp. 143-146.

Roberts N, Black S, Boyer B, Eastwood WJ, Griffths HI, Lamb HF, Leng MJ, Parish R, Reed JM, Twigg D, Yigitbasioglu H (1999). Chronology and stratigraphy of late quaternary sediments in the Konya Basin, Turkey: results from the KOPAL project. Quat Sci Rev 18: 611-630.

Salman M, Akyıldız M (2013). Investigation of geological and chemical properties of lignites around Ayrancı (Karaman) and Karapınar (Konya). Çukurova Univ J Fac Engin Architect 28: 133-140 (in Turkish with an abstract in English).

Schildgen TF, Yıldırım C, Cosentino D, Strecker MR (2014). Linking slab break-off, Hellenic trench retreat, and uplift of the central and eastern Anatolian plateaus. Earth Sci Rev 128: 147-168.

Scott AC (2002). Coal petrology and the origin of coal macerals: a way ahead? Int J Coal Geol 50: 119-134.

Siavalas G, Linou M, Chatziapostolou A, Kalaitzidis S, Papaefthymiou H, Christanis K (2009). Palaeoenvironment of Seam I in the Marathousa Lignite Mine, Megalopolis Basin (Southern Greece). Int J Coal Geol 78: 233-248.

Silva MB, Kalkreuth W, Holz M (2008). Coal petrology of coal seams from the Leão-Butiá Coalfield, Lower Permian of the Paraná Basin, Brazil - Implications for coal facies interpretations. Int J Coal Geol 73: 331-358.

Singh MP, Singh AK (2000). Petrographic characteristics and depositional conditions Eocene coals of platform basins, Meghalaya, India. Int J Coal Geol 45: 315-356.

Stout, SA, Spackman W (1989). Peatification and early coalification of wood as deduced by quantitative microscopic methods. Org Geochem 14: 285-298.

Suárez-Ruiz I, Jimenez A, Iglesias J, Laggoun-Defarge F, Pradot JG (1994). Influence of resinite on huminite properties. Energ Fuel 8: 1417-1424.

Sýkorová I, Pickel W, Christanis K, Wolf M, Taylor GH, Flores D (2005). Classification of huminite - ICCP System 1994. Int J Coal Geol 62: 85-106.

Temiz U, Savaş F (2014). Relationship between Akhüyük fissure ridge travertines and active tectonics: Their neotecteonic significance (Ereğli-Konya, central Anatolia). Arab J Geosci 8: 2383-2392.

Toprak V, Göncüoğlu MC (1993). Tectonic control on the development of the Neogene-Quaternary central Anatolia Volcanic Province, Turkey. Geol J 28: 357-369.

Ulu Ü, Öcal H, Bulduk AK, Karakaş M, Arbas A, Saçlı L, Taşkıran MA, Ekmekçi E, Adır M, Sözeri Ş, Karabıyıkoğlu M (1994). Late Cenozoic depositional system surrounding area of Cihanbeyli-Karapınar. This tectonic and climatic importance. Bull Geol Cong Turkey 9: 149-163 (in Turkish with an English abstract).

Ward CR (2002). Analysis and significance of mineral matter in coal seams. Int J Coal Geol 50: 135-168.

Ward CR (2016). Analysis, origin and significance of mineral matter in coal: An updated review. Int J Coal Geol 165: 1-27.

Wüst RAJ, Hawke MI, Bustin MR (2001). Comparing maceral ratios from tropical peatlands with assumptions from coal studies: do classic coal petrographic interpretation methods have to be discarded? Int J Coal Geol 48: 115-132.

Zdravkov A, Bechtel A, Sachsenhofer RF, Kortenski J, Gratzer R (2011). Vegetation differences and diagenetic changes between two Bulgarian lignite deposits - Insights from coal petrology and biomarker composition. Org Geochem 42: 237-254.